Annals of Physics 378 (2017) 33–46

Contents lists available at ScienceDirect

Annals of Physics

journal homepage: www.elsevier.com/locate/aop

# Heralded quantum repeater based on the scattering of photons off single emitters in one-dimensional waveguides

Guo-Zhu Song [a], Mei Zhang [a], Qing Ai [a], Guo-Jian Yang [a], Ahmed Alsaedi [b], Aatef Hobiny [b], Fu-Guo Deng [a,b,*]

[a] *Department of Physics, Applied Optics Beijing Area Major Laboratory, Beijing Normal University, Beijing 100875, China*

[b] *NAAM-Research Group, Department of Mathematics, Faculty of Science, King Abdulaziz University, P.O. Box 80203, Jeddah 21589, Saudi Arabia*

ARTICLE INFO

*Article history:*
Received 13 June 2016
Accepted 8 January 2017
Available online 10 January 2017

*Keywords:*
Heralded quantum repeater
One-dimensional waveguides
Scattering property
Atom-waveguide systems

ABSTRACT

We propose a heralded quantum repeater based on the scattering of photons off single emitters in one-dimensional waveguides. We show the details by implementing nonlocal entanglement generation, entanglement swapping, and entanglement purification modules with atoms in waveguides, and discuss the feasibility of the repeater with currently achievable technology. In our scheme, the faulty events can be discarded by detecting the polarization of the photons. That is, our protocols are accomplished with a fidelity of 100% in principle, which is advantageous for implementing realistic long-distance quantum communication. Moreover, additional atomic qubits are not required, but only a single-photon medium. Our scheme is scalable and attractive since it can be realized in solid-state quantum systems. With the great progress on controlling atom-waveguide systems, the repeater may be very useful in quantum information processing in the future.



* Corresponding author at: Department of Physics, Applied Optics Beijing Area Major Laboratory, Beijing Normal University, Beijing 100875, China.
*E-mail address:* fgdeng@bnu.edu.cn (F.-G. Deng).

http://dx.doi.org/10.1016/j.aop.2017.01.007
0003-4916/

## 1. Introduction

Entanglement plays an important role in quantum communication, such as quantum key distribution [1,2], quantum secret sharing [3], and quantum secure direct communication [4,5]. However, entangled photon pairs are produced locally and inevitably suffer from the noise from optical-fiber channels when they are transmitted to the parties in quantum communication, which will decrease the coherence of the photon systems. In order to exchange private information and avoid an exponential decay of photons over long distance, the scheme for a quantum repeater was proposed by Briegel et al. [6] in 1998. Its main idea is to share the entangled photon pairs in small segments first, avoiding the exponential decay of photons with the transmission distance, and then use entanglement swapping [7] and entanglement purification [8–18] to create a long-distance entangled quantum channel.

There are some interesting proposals for implementing a quantum repeater, by utilizing different physical systems [19–23]. For example, in 2001, Duan et al. [19] suggested an interesting proposal to set up a quantum repeater with atomic ensembles. In 2006, Klein et al. [20] put forward a robust scheme for quantum repeaters with decoherence-free subspaces. In 2007, using the two-photon Hong-Ou-Mandel interferometer, Zhao et al. [21] proposed a robust quantum repeater protocol. In 2016, Li, Yang, and Deng [22] introduced a heralded quantum repeater for quantum communication network based on quantum dots embedded in optical microcavities, resorting to effective time-bin encoding. The building blocks of quantum repeaters are experimentally realized by some research groups, and remarkable progress has been reported [24–28].

In the past decade, the interaction between photons and atoms in high-quality optical microcavities has become one of the most important methods for implementing quantum computation and quantum information processing. Some significant achievements [29–33] have been made in photon–atom systems in both theory and experiment. With strong coupling and high-quality cavities, they can obtain a high-fidelity quantum computation. In 2005, an interesting proposal [34] was proposed to realize the coupling between a single quantum emitter and a photon in one-dimensional (1D) waveguides, which can be considered as a bad cavity. In 2007, a similar proposal was presented to realize this coupling using nanoscale surface plasmons [35]. In 2015, Söllner et al. [36] obtained deterministic photon–emitter coupling in photonic crystal waveguide in experiment. In their schemes, the coupling between an emitter and a 1D waveguide is stronger than the atomic decay rate, but weaker than the waveguide-loss rate, and the atomic spontaneous emission into the waveguide becomes the main effect, called the Purcell effect. The emitter–waveguide systems allow for interesting quantum state manipulation and quantum information processing, such as entanglement generation [37–39], efficient optical switch [40], quantum logic gates [41,42], and quantum state transfer [43–45]. However, with emitter decay and finite coupling strength, the physical device is restricted to finite $P$ (Purcell factor), so that the scattering of photons off single emitters may not happen at all. To solve this problem, in 2012, Li et al. [43] proposed a simple scattering setup to realize a robust-fidelity atom–photon entangling gate, in which the faulty events can be heralded by detecting the polarization of the photon pulse.

In this paper, we present a heralded quantum repeater that allows the nonlocal creation of the entangled state over an arbitrary large distance with a tolerability of errors. In our scheme, since atoms can provide long coherence time, we choose a four-level atom as the emitter. With the scattering of photons off single emitters in 1D waveguides, the parties in quantum communication can realize nonlocal entanglement creation against collective noise, entanglement swapping, and entanglement purification. Moreover, our protocols can turn errors into the detection of photon polarization, which can be discarded. The prediction of faulty events ensures that our repeater can be completed with a fidelity of 100% in principle, which is advantageous for quantum information processing.

## 2. The scattering of photons off single emitters in a 1D waveguide

Let us consider a quantum system composed of a single emitter coupled to electromagnetic modes in a 1D waveguide, as shown in Fig. 1(a). We first choose a simple two-level atom as the emitter, consisting of the ground state $|g\rangle$ and the excited state $|e\rangle$ with the frequency difference $\omega_a$. Under

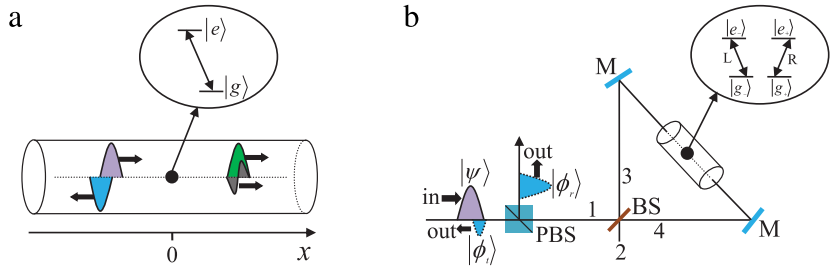


**Fig. 1.** (Color online) (a) The basic structure for a photon mirror in which a two-level atom (an emitter marked by the black dot) is coupled to a 1D waveguide (marked by the cylinder). Here the atom has a ground state $|g\rangle$ and an excited state $|e\rangle$, and its position is $x = 0$. In an ideal situation, an incident photon (purple, the upper left wave packet) is fully reflected (blue, the lower left wave packet) when it resonates with the atom, but there is a transmitted component (black, the right wave packet) in a practical scattering [35]. Note that, when the incident photon is detuned from the emitter, it goes through the atom with no effect (green, the upper right wave packet). (b) A heralded setup to realize the scattering between the photon and emitter in a 1D waveguide [43]. Different from the emitter in Fig. 1(a), the atom has two degenerate ground states $|g_\pm\rangle$ and two degenerate excited states $|e_\pm\rangle$ coupled to the waveguide (marked by the cylinder). *PBS* represents a polarizing beam splitter which transmits the horizontal polarized photon $|H\rangle$ and reflects the vertical polarized photon $|V\rangle$, BS is a $50:50$ beam splitter, $M$ is a fully reflected mirror, and the black lines represent the paths of the traveling photon.

the Jaynes–Cummings model, the Hamiltonian for the interactions between a set of waveguide modes and a two-level emitter reads [34,35]:

$$H = \sum_k \hbar\omega_k a_k^\dagger a_k + \frac{1}{2}\hbar\omega_a\sigma_z + \sum_k \hbar g(a_k^\dagger\sigma_- + a_k\sigma_+), \tag{1}$$

where $a_k$ and $a_k^\dagger$ are the annihilation and creation operators of the waveguide mode with frequency $\omega_k$, respectively. $\sigma_z$, $\sigma_+$, and $\sigma_-$ are the inversion, raising, and lowering operators of the two-level atom, respectively. $g$ is the coupling strength between the atom and the electromagnetic modes of the 1D waveguide, assumed to be same for all modes. One can rewrite the Hamiltonian of the system in real space as [34,35]

$$H' = \hbar\int dk\,\omega_k a_k^\dagger a_k + \hbar g\int dk(a_k\sigma_+ e^{ikx_a} + h.c.) + \hbar\left(\omega_a - \frac{i\gamma'}{2}\right)\sigma_{ee}, \tag{2}$$

where $x_a$ is the position of the atom, $\sigma_{ee} = |e\rangle\langle e|$, and $\omega_k = c|k|$ ($c$ is the group velocity of propagating electromagnetic modes and $k$ is its wave vector). $\gamma'$ is the decay rate of the atom out of the waveguide (e.g., the emission into the free space). Because we only care the interactions of the near-resonant photons with the atom, we could make the approximation that left- and right-propagating photons form completely separate quantum fields [34]. Under this approximation, the operator $a_k$ in Eq. (2) can be replaced by $(a_{k,R} + a_{k,L})$.

To get the reflection and transmission coefficients of single-photon scattering, we assume that a photon with the energy $E_k$ is propagating from the left. The state of the system is described by [34,35]

$$|E_k\rangle = c_e|e, vac\rangle + \int dx\left[\phi_L(x)c_L^\dagger(x) + \phi_R(x)c_R^\dagger(x)\right]|g, vac\rangle, \tag{3}$$

where $|vac\rangle$ represents the vacuum state of photons, $c_e$ is the probability amplitude of the atom in the excited state, and $c_L^\dagger(x)$ ($c_R^\dagger(x)$) is a bosonic operator creating a left-going (right-going) photon at position $x$. $\phi_R(x)$ and $\phi_L(x)$ are the probability amplitudes of right- and left-traveling photons, respectively. Note that the photon propagates from the left, $\phi_R(x)$ and $\phi_L(x)$ could take the forms [34,35]

$$\begin{aligned}\phi_R(x) &= e^{ikx}\theta(-x) + te^{ikx}\theta(x),\\ \phi_L(x) &= re^{-ikx}\theta(-x).\end{aligned} \tag{4}$$

Here $t$ and $r$ are the transmission and reflection coefficients, respectively. The Heaviside step function $\theta(x)$ equals 1 when $x$ is larger than zero and 0 when $x$ is smaller than zero. By solving the

time-independent Schrödinger equation $H|E_k\rangle = E_k|E_k\rangle$, one can obtain [34,35]

$$r = -\frac{1}{1+\gamma'/\gamma_{1D} - 2i\Delta/\gamma_{1D}},$$
$$t = 1 + r, \tag{5}$$

where $\Delta = \omega_k - \omega_a$ is the photon detuning with the two-level atom, and $\gamma_{1D} = 4\pi g^2/c$ is the decay rate of the atom into the waveguide.

Provided that the incident photon resonates with the emitter (i.e., $\Delta = 0$), one can easily obtain the reflection coefficient $r = -1/(1 + 1/P)$, where $P = \gamma_{1D}/\gamma'$ is the Purcell factor. As we know, in the atom-waveguide system, the spontaneous emission rate $\gamma_{1D}$ into the 1D waveguide can be much larger than the emission rate $\gamma'$ into all other possible channels [34,35]. Considering that a high Purcell factor $P$ can be obtained in realistic systems [35], one can get the reflection coefficient $r \approx -1$ for this system in principle. That is, when the photon is coupled to the emitter, the atom acts as a photon mirror [34], which puts a $\pi$-phase shift on reflection. However, when the photon is detuned from the emitter, it transmits through the atom with no effect.

Let us consider a four-level atom with degenerate ground states $|g_\pm\rangle$ and excited states $|e_\pm\rangle$ as the emitter in a 1D waveguide, as shown in Fig. 1(b). For the emitter, the transitions of $|g_+\rangle \leftrightarrow |e_+\rangle$ and $|g_-\rangle \leftrightarrow |e_-\rangle$ are coupled to two electromagnetic modes $a_{k,R}$ and $a_{k,L}$, with the absorption (or emission) of right ($R$) and left ($L$) circular polarization photons, respectively. Assuming that the spatial wave function of the incident photon is $|\psi\rangle$, with the scattering properties in the practical situation discussed above, one can get [43]

$$\begin{aligned} &|g_+\rangle\,|\psi\rangle\,|R\rangle \to |g_+\rangle\,|\phi\rangle\,|R\rangle, \qquad |g_-\rangle\,|\psi\rangle\,|R\rangle \to |g_-\rangle\,|\psi\rangle\,|R\rangle,\\ &|g_-\rangle\,|\psi\rangle\,|L\rangle \to |g_-\rangle\,|\phi\rangle\,|L\rangle, \qquad |g_+\rangle\,|\psi\rangle\,|L\rangle \to |g_+\rangle\,|\psi\rangle\,|L\rangle. \end{aligned} \tag{6}$$

Here $|\phi\rangle$ is the spatial state of the photon component left in the waveguide after the scattering process. In general situation, $|\phi\rangle = |\phi_t\rangle + |\phi_r\rangle$, where $|\phi_t\rangle = t|\psi\rangle$ and $|\phi_r\rangle = r|\psi\rangle$ refer to the transmitted and reflected parts of the photon, respectively. When the Purcell factor $P$ is infinite, $|\phi\rangle$ is normalized. Whereas, if the input photon is in the horizontal linear-polarization state $|H\rangle = (|R\rangle + |L\rangle)/\sqrt{2}$, the transformations turn into [43]

$$\begin{aligned} |g_+\rangle|\psi\rangle\,|H\rangle &\to \frac{1}{2}|g_+\rangle[(|\phi\rangle + |\psi\rangle)|H\rangle + (|\phi\rangle - |\psi\rangle)|V\rangle],\\ |g_-\rangle\,|\psi\rangle|H\rangle &\to \frac{1}{2}|g_-\rangle[(|\phi\rangle + |\psi\rangle)|H\rangle - (|\phi\rangle - |\psi\rangle)|V\rangle], \end{aligned} \tag{7}$$

where $|V\rangle = (|R\rangle - |L\rangle)/\sqrt{2}$ is the vertical linear-polarization state. Following the relation in Eq. (5), one gets $(|\phi\rangle + |\psi\rangle)/2 = |\phi_t\rangle$ and $(|\phi\rangle - |\psi\rangle)/2 = |\phi_r\rangle$ [43], and the transformations in Eq. (7) are equivalent to

$$\begin{aligned} &|g_+\rangle\,|\psi\rangle\,|H\rangle \to |g_+\rangle\,|\phi_t\rangle\,|H\rangle + |g_+\rangle\,|\phi_r\rangle\,|V\rangle,\\ &|g_-\rangle\,|\psi\rangle\,|H\rangle \to |g_-\rangle\,|\phi_t\rangle\,|H\rangle - |g_-\rangle\,|\phi_r\rangle\,|V\rangle. \end{aligned} \tag{8}$$

It is interesting that the scattering process generates a vertical-polarized component. Moreover, for the outgoing photon in state $|H\rangle$, nothing happens to the emitter, while for the photon component in state $|V\rangle$, a state-dependent $\pi$- phase shift occurs on the emitter.

With the principle mentioned above, Li et al. [43] constructed a heralded setup to realize the scattering between incident photon and the emitter in a 1D waveguide, as shown in Fig. 1(b). The input photon in spatial state $|\psi\rangle$ with $|H\rangle$ (from port 1) is split by a 50 : 50 beam splitter (BS) into two halves that scatter with the atom simultaneously. Then, the transmitted and reflected components travel back and exit the beam splitter from port 1. The corresponding transformations on the states can be described as follows [43]:

$$\begin{aligned} |\Phi_0\rangle &= |g_\pm\rangle\,|\psi\rangle\,|H\rangle^1\\ &\xrightarrow{BS} \frac{1}{\sqrt{2}}|g_\pm\rangle\,|\psi\rangle\,|H\rangle^3 + \frac{1}{\sqrt{2}}|g_\pm\rangle\,|\psi\rangle\,|H\rangle^4 \end{aligned}$$

$$\xrightarrow{Scatter} \frac{1}{\sqrt{2}}|g_{\pm}\rangle\,|\phi_t\rangle\,|H\rangle^{3} + \frac{1}{\sqrt{2}}|g_{\pm}\rangle\,|\phi_t\rangle\,|H\rangle^{4} \pm \frac{1}{\sqrt{2}}|g_{\pm}\rangle\,|\phi_r\rangle\,|V\rangle^{3} \pm \frac{1}{\sqrt{2}}|g_{\pm}\rangle\,|\phi_r\rangle\,|V\rangle^{4}$$
$$\xrightarrow{BS} |g_{\pm}\rangle\,|\phi_t\rangle|H\rangle^{1} \pm |g_{\pm}\rangle\,|\phi_r\rangle\,|V\rangle^{1}. \quad (9)$$

Here the superscript $i$ ($i = 1, 2, 3, 4$) is the path of the photon, shown in Fig. 1(b).

Note that, due to quantum destructive interference, there is no photon component coming out from port 2. Finally, with the help of *PBS*, discarding the horizontal polarization output from Eq. (9) (i.e., the faulty event), one can get the transformations as follows [43]:

$$|g_-\rangle\,|\psi\rangle\,|H\rangle \to -|g_-\rangle\,|\phi_r\rangle\,|V\rangle,$$
$$|g_+\rangle\,|\psi\rangle\,|H\rangle \to +|g_+\rangle\,|\phi_r\rangle\,|V\rangle. \quad (10)$$

Similarly, when the incident photon is in state $|V\rangle$, discarding the faulty event with vertical polarization output, the transformations are described as follows [43]:

$$|g_-\rangle\,|\psi\rangle\,|V\rangle \to -|g_-\rangle\,|\phi_r\rangle\,|H\rangle,$$
$$|g_+\rangle\,|\psi\rangle\,|V\rangle \to +|g_+\rangle\,|\phi_r\rangle\,|H\rangle. \quad (11)$$

As mentioned above, $|\phi_r\rangle$ is the spatial wave function of the reflected photon component after the scattering process. When $P \to \infty$, the perfect scattering process leads to $|\phi_r\rangle = -|\psi\rangle$. In the imperfect situation with a finite $P$, there is always a transmitted part [35], we get $|\phi_r\rangle \neq -|\psi\rangle$, the output photon with unchanged polarization is detected and the corresponding scattering event fails, which can be discarded. That is, the setup for realizing the scattering event between incident photon and the emitter works in a heralded way.

## 3. Quantum repeater based on the scattering configuration

### 3.1. Robust nonlocal entanglement creation against collective noise

With the property of a photon scattering with a four-level atom coupled to a 1D waveguide, we can design a robust scheme for the entanglement creation on two nonlocal stationary atoms $a$ and $b$, as shown in Fig. 2. Suppose that the single photon medium and the two stationary atoms in 1D waveguides are initially prepared in the superposition states $|\psi_0\rangle^p = \frac{1}{\sqrt{2}}(|H\rangle + |V\rangle)$ and $|\varphi_i\rangle = \frac{1}{\sqrt{2}}(|0\rangle + |1\rangle)_i$ (here $|0\rangle = |g_-\rangle$, $|1\rangle = |g_+\rangle$, $i = a, b$), respectively, the state of the system composed of the photon and the two atoms is

$$|\Omega_0\rangle = \frac{1}{2\sqrt{2}}(|H\rangle + |V\rangle) \otimes (|0\rangle + |1\rangle)_a \otimes (|0\rangle + |1\rangle)_b. \quad (12)$$

Our scheme works with the following steps.

First, the $|H\rangle$ and $|V\rangle$ components of the input photon are spatially split by a polarizing beam splitter (*PBS*). In detail, the photon in state $|H\rangle$ passes through both $PBS_1$ and $PBS_2$ towards the setup to scatter with atom $a$. While the component in state $|V\rangle$ is reflected into the other arm of the interferometer by $PBS_1$, and is reflected by $TR_1$ into the channel, having no interaction with atom $a$. After the scattering process, the part interacting with atom $a$ travels through $TR_1$ into the channel, but a little later than the other part. The state of the whole system at the entrance of the channel becomes $|\Omega_1\rangle$. Here

$$|\Omega_1\rangle = |\Omega_{1S}\rangle + |\Omega_{1L}\rangle,$$
$$|\Omega_{1S}\rangle = \frac{1}{2\sqrt{2}}|V\rangle_S \otimes (|0\rangle + |1\rangle)_a \otimes (|0\rangle + |1\rangle)_b,$$
$$|\Omega_{1L}\rangle = \frac{1}{2\sqrt{2}}|V\rangle_L \otimes (|0\rangle - |1\rangle)_a \otimes (|0\rangle + |1\rangle)_b, \quad (13)$$

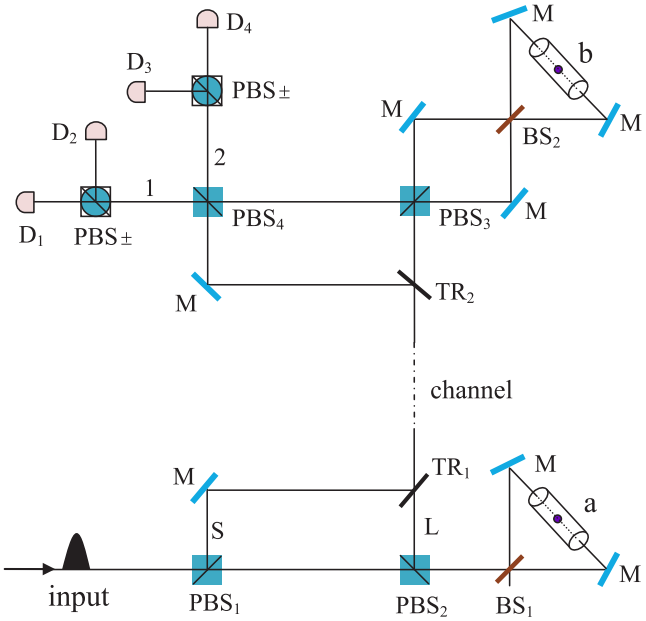


**Fig. 2.** (Color online) Schematic setup for the creation of maximally entangled states on two nonlocal atoms $a$ and $b$ in 1D waveguides. $PBS\pm$ transmits photons with polarization $|+\rangle$ and reflects photons with polarization $|-\rangle$, where $|\pm\rangle = (1/\sqrt{2})(|H\rangle \pm |V\rangle)$. $D_i$ $(i = 1, 2, \ldots, 4)$ is a photon detector and $TR_i$ $(i = 1, 2)$ is an optical device which can be controlled exactly as needed to transmit or reflect a photon.

where $|\Omega_{1S}\rangle$ and $|\Omega_{1L}\rangle$ represent the two parts of the photon going through the short path ($S$) and the long path ($L$) to the channel, respectively.

Second, as the two parts in the channel are near and their polarization states are both in $|V\rangle$, the influences of the collective noise in the quantum channel on these two parts are the same one [46–48], which can be described by $|V\rangle \rightarrow \gamma|V\rangle + \delta|H\rangle$, where $|\gamma|^2 + |\delta|^2 = 1$. After the photon travels in the long quantum channel, the state of the whole system at the output port becomes

$$\begin{aligned}
|\Omega_2\rangle &= |\Omega_{2S}\rangle + |\Omega_{2L}\rangle,\\
|\Omega_{2S}\rangle &= \frac{1}{2\sqrt{2}}(\gamma|V\rangle_S + \delta|H\rangle_S)(|0\rangle + |1\rangle)_a(|0\rangle + |1\rangle)_b,\\
|\Omega_{2L}\rangle &= \frac{1}{2\sqrt{2}}(\gamma|V\rangle_L + \delta|H\rangle_L)(|0\rangle - |1\rangle)_a(|0\rangle + |1\rangle)_b.
\end{aligned} \tag{14}$$

Third, getting out from the noisy channel, the early part of the photon in state $|\Omega_{2S}\rangle$ is reflected by the optical device $TR_2$, while the late part in state $|\Omega_{2L}\rangle$ transmits through $TR_2$ into $PBS_3$. After that, the components in states $|H\rangle$ and $|V\rangle$ of the late part are split into two halves that scatter with atom $b$ and travel back to $PBS_3$ simultaneously. Subsequently, the early part and the late part are rejoined in $PBS_4$, and they are separated into two paths 1 and 2. The state of the whole system evolves into

$$\begin{aligned}
|\Omega_3\rangle = {} & \frac{1}{2\sqrt{2}}\gamma(|H\rangle + |V\rangle)_1(|0\rangle\,|0\rangle + |1\rangle\,|1\rangle)_{ab} - \frac{1}{2\sqrt{2}}\gamma(|H\rangle - |V\rangle)_1(|0\rangle\,|1\rangle + |1\rangle\,|0\rangle)_{ab}\\
& + \frac{1}{2\sqrt{2}}\delta(|H\rangle + |V\rangle)_2(|0\rangle\,|0\rangle + |1\rangle\,|1\rangle)_{ab} + \frac{1}{2\sqrt{2}}\delta(|H\rangle - |V\rangle)_2(|0\rangle\,|1\rangle + |1\rangle\,|0\rangle)_{ab}.
\end{aligned} \tag{15}$$

Finally, the two parts in paths 1 and 2 go through $PBS\pm$, and the photon is detected by one of the four single-photon detectors $D_1$, $D_2$, $D_3$, and $D_4$. If the detector $D_2$ or $D_3$ clicks, we should put

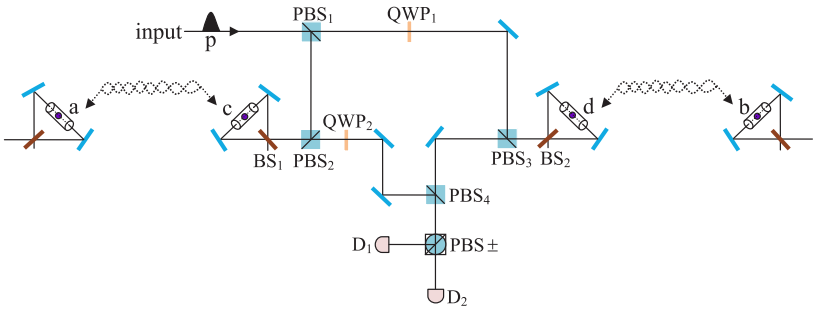


**Fig. 3.** (Color online) Schematic diagram showing the principle of entanglement swapping. $QWP_i$ $(i = 1, 2)$ represents a quarter-wave plate, which is used to implement the conversion of the photon polarization.

a $\sigma_x$ operation on atom $b$. If the detector $D_1$ or $D_4$ clicks, nothing needs to be done. Eventually, the state of the system composed of atoms $a$ and $b$ collapses to the maximally entangled state $|\phi^+\rangle_{ab} = \frac{1}{\sqrt{2}}(|0\rangle|0\rangle + |1\rangle\,|1\rangle)_{ab}$.

Note that, for successful events of imperfect processes, i.e., with finite $P$, the polarization is swapped but $|\phi_r\rangle \neq -|\psi\rangle$ in Eqs. (10) and (11). This causes a problem that the spatial wave functions in two arms of the interferometer are not matched at $PBS_4$. To overcome the unbalance between the two spatial wave functions, a waveform corrector (*WFC*) is adopted in one arm of the interferometer. In fact, the *WFC* can be realized by a second scattering module, which is identical to that of Fig. 1(b). In detail, we make the auxiliary emitter in *WFC* permanently stay in $|g_-\rangle$, before and after the scattering process, a quarter wave plate is needed to implement $|V\rangle \leftrightarrow |L\rangle$. With the waveform correctors, the corresponding wave packet is changed from $|\psi\rangle$ to $|\phi_r\rangle$ without entangling with the auxiliary emitter. The *WFC* decreases the overall success probability of the entanglement creation, but not affect the fidelity in principle.

Our setup for the robust entanglement creation on two nonlocal atoms has some interesting features. First, the early part and the late part of the photon in the channel are so near that they suffer from the same collective noise [46–48], and an arbitrary qubit error caused by the long noisy channel can be perfectly settled, i.e., as shown in Eq. (15), the probability of the entanglement creation does not depend on the values of collective noise parameters $\gamma$ and $\delta$. Second, the faulty interactions between the photon and two atoms can be heralded by the detectors $D_1$, $D_2$, $D_3$, and $D_4$. In detail, if none of these detectors clicks, the event of the entanglement creation fails, which can be discarded. These good features make our setup have good applications in quantum repeaters for long-distance quantum communication.

### 3.2. Entanglement swapping

The atomic entangled state can be connected to longer communication distance via local entanglement swapping. Inspired by the recent work [49], we construct the entanglement swapping scheme, using the scattering of a single photon combined with measurements on the atoms, as shown in Fig. 3. The two pairs of nonlocal atoms $ac$ and $bd$ are both initially prepared in the maximally entangled states $|\phi^+\rangle_{ac} = \frac{1}{\sqrt{2}}(|0\rangle|0\rangle+|1\rangle|1\rangle)_{ac}$ and $|\phi^+\rangle_{bd} = \frac{1}{\sqrt{2}}(|0\rangle|0\rangle+|1\rangle|1\rangle)_{bd}$, respectively. With the Bell-state measurement on local atoms $cd$ and single-qubit operations, the two nonlocal atoms $ab$ can collapse to the maximally entangled state $|\phi^+\rangle_{ab} = \frac{1}{\sqrt{2}}(|0\rangle|0\rangle+|1\rangle|1\rangle)_{ab}$, which indicates that the nonlocal entanglement for a longer communication is realized. The principle of quantum swapping is shown in Fig. 3, and the details are described as follows.

First, suppose that the input photon $p$ is prepared in the superposition state $|\psi_0\rangle^p = \frac{1}{\sqrt{2}}(|H\rangle+|V\rangle)$, and the initial state of the whole system composed of photon $p$ and the four atoms $acbd$ is $|\Psi_0\rangle$. Here,

$$|\Psi_0\rangle = \frac{1}{2\sqrt{2}}(|H\rangle + |V\rangle) \otimes (|0\rangle\,|0\rangle + |1\rangle\,|1\rangle)_{ac} \otimes (|0\rangle\,|0\rangle + |1\rangle\,|1\rangle)_{bd}. \tag{16}$$

**Table 1**
The operations on atom $a$ corresponding to the outcomes of the photon detectors and the states of atoms $cd$.

| Photon click | Atom $c$ | Atom $d$ | Operations on atom $a$ |
|---|---|---|---|
| $D_1$ | $\|0\rangle(\|1\rangle)$ | $\|1\rangle(\|0\rangle)$ | $I$ |
| $D_1$ | $\|0\rangle(\|1\rangle)$ | $\|0\rangle(\|1\rangle)$ | $\sigma_z$ |
| $D_2$ | $\|0\rangle(\|1\rangle)$ | $\|1\rangle(\|0\rangle)$ | $\sigma_x$ |
| $D_2$ | $\|0\rangle(\|1\rangle)$ | $\|0\rangle(\|1\rangle)$ | $\sigma_z\sigma_x$ |

The injecting photon $p$ passes through $PBS_1$, which transmits the photon in state $|H\rangle$ and reflects the photon in state $|V\rangle$. The photon in state $|V\rangle$ is reflected by $PBS_1$ and $PBS_2$ into the scattering setup composed of atom $c$, while the other part in state $|H\rangle$ goes through $QWP_1$ and is reflected by $PBS_3$ into the scattering setup to scatter with atom $d$. Then, the two parts of the photon $p$ are rejoined in $PBS_4$. After that, the state of the whole system is changed from $|\Psi_0\rangle$ to $|\Psi_1\rangle$. Here,

$$\begin{aligned}|\Psi_1\rangle = & \frac{(|H\rangle+|V\rangle)}{4\sqrt{2}}\big[(|00\rangle-|11\rangle)_{cd}\otimes(|00\rangle+|11\rangle)_{ab}+(|00\rangle+|11\rangle)_{cd}\otimes(|00\rangle-|11\rangle)_{ab}\big]\\ & -\frac{(|H\rangle-|V\rangle)}{4\sqrt{2}}\big[(|01\rangle-|10\rangle)_{cd}\otimes(|01\rangle+|10\rangle)_{ab}+(|01\rangle+|10\rangle)_{cd}\\ & \otimes(|01\rangle-|10\rangle)_{ab}\big].\end{aligned} \tag{17}$$

Second, a Hadamard operation $H_a$ (e.g., using a $\pi/2$ microwave pulse or optical pulse [50,51]) is performed on the two local atoms $c$ and $d$ in the waveguides, respectively. Then, the state of the whole system becomes

$$\begin{aligned}|\Psi_2\rangle = & \frac{(|H\rangle+|V\rangle)}{4\sqrt{2}}\big[(|01\rangle+|10\rangle)_{cd}\otimes(|00\rangle+|11\rangle)_{ab}+(|00\rangle+|11\rangle)_{cd}\otimes(|00\rangle-|11\rangle)_{ab}\big]\\ & +\frac{(|H\rangle-|V\rangle)}{4\sqrt{2}}\big[(|01\rangle-|10\rangle)_{cd}\otimes(|01\rangle+|10\rangle)_{ab}-(|00\rangle-|11\rangle)_{cd}\\ & \otimes(|01\rangle-|10\rangle)_{ab}\big].\end{aligned} \tag{18}$$

Then, the photon $p$ travels through $PBS\pm$ and is detected by single-photon detectors. Meanwhile, the state of atom $c$ ($d$) is measured by external classical field.

Third, with the outcomes of the detectors for photon $p$ and the measurements on atoms $cd$, one can see that the four Bell states of the atoms $a$ and $b$ are completely distinguished. Finally, the parties can perform corresponding operations (see Table 1) on atom $a$ to complete the quantum swapping. After that, the state of the two nonlocal atoms $a$ and $b$ in a longer distance collapses to the maximally entangled state $|\phi^+\rangle_{ab}=\frac{1}{\sqrt{2}}(|0\rangle\,|0\rangle+|1\rangle\,|1\rangle)_{ab}$.

It is important to note that the wrong interactions between photon and atoms are heralded by the photon detectors in our protocol. In detail, if neither of the detectors $D_1$ and $D_2$ clicks, the interactions between photon and two atoms in 1D waveguides are faulty, which could be discarded. Therefore, with the prediction of the faulty events, the parties can obtain a high-fidelity nonlocal atomic entangled state in a longer distance.

### 3.3. Entanglement purification

In Sections 3.1 and 3.2, we just talk about the influence of noise on flying photons in long quantum channel. In the practical situation, the errors also occur in stationary atoms embedded in 1D waveguides, which will decrease the entanglement of the nonlocal two-atom systems. Using entanglement purification [8–18], we can distill some high-fidelity maximally entangled states from a mixed entangled state ensemble. Now, we start to explain the principle of our purification protocol for nonlocal atomic entangled states, assisted by the scattering of photons off single atoms in 1D waveguides, as shown in Fig. 4.

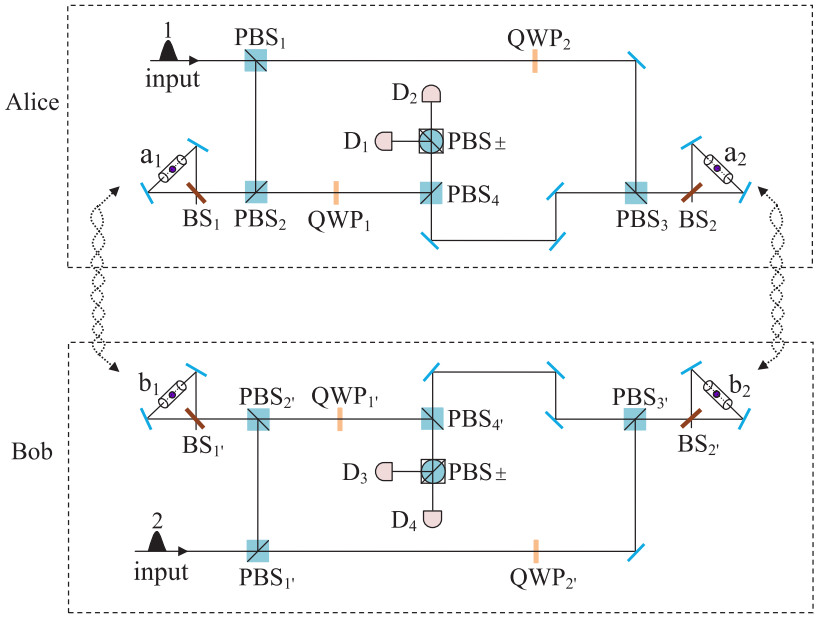


**Fig. 4.** (Color online) Schematic setup showing the principle of the atomic entanglement purification protocol based on the scattering of photons off single emitters.

Suppose that the initial mixed state shared by two remote parties, say Alice and Bob, can be written as

$$\rho_{ab} = F|\phi^+\rangle_{ab}\langle\phi^+| + (1-F)|\psi^+\rangle_{ab}\langle\psi^+|, \tag{19}$$

where $|\psi^+\rangle_{ab} = \frac{1}{\sqrt{2}}(|0\rangle|1\rangle + |1\rangle|0\rangle)_{ab}$. The subscripts $a$ and $b$ represent the single atoms in 1D waveguides owned by Alice and Bob, respectively. $F$ is the initial fidelity of the state $|\phi^+\rangle$. By selecting two pairs of nonlocal entangled two-atom systems, the four atoms are in the states $|\phi^+\rangle_{a_1b_1}|\phi^+\rangle_{a_2b_2}$ with the probability of $F^2$, $|\phi^+\rangle_{a_1b_1}|\psi^+\rangle_{a_2b_2}$ and $|\psi^+\rangle_{a_1b_1}|\phi^+\rangle_{a_2b_2}$ with a probability of $F(1-F)$, and $|\psi^+\rangle_{a_1b_1}|\psi^+\rangle_{a_2b_2}$ with a probability of $(1-F)^2$, respectively. Our entanglement purification protocol for nonlocal entangled atom pairs works with the following steps.

First, both Alice and Bob prepare an optical pulse in the superposition state $\frac{1}{\sqrt{2}}(|H\rangle + |V\rangle)$ and let them pass through the equipments shown in Fig. 4. Here, we choose the case $|\phi^+\rangle_{a_1b_1}|\phi^+\rangle_{a_2b_2}$ to illustrate the principle. To simplify the discussion, we just discuss the interactions in Alice, and Bob need complete the same process simultaneously. For Alice, the $|H\rangle$ and $|V\rangle$ components of the input photon 1 are spatially split by $PBS_1$. In detail, the component in $|V\rangle$ is reflected by both $PBS_1$ and $PBS_2$ to the scattering setup composed of atom $a_1$, whereas the component in $|H\rangle$ goes through $QWP_2$ and is reflected by $PBS_3$ to the scattering setup containing atom $a_1$. After that, the state of the whole system is changed from $|\Phi_0\rangle$ to $|\Phi_1\rangle$, where

$$\begin{aligned}
|\Phi_0\rangle &= \frac{1}{2}(|H\rangle + |V\rangle)_1\ (|H\rangle + |V\rangle)_2\ |\phi^+\rangle_{a_1b_1}|\phi^+\rangle_{a_2b_2},\\
|\Phi_1\rangle &= \frac{1}{4}|H\rangle_1\,(|H\rangle + |V\rangle)_2 \otimes (|0000\rangle - |0011\rangle + |1100\rangle - |1111\rangle)_{a_1b_1a_2b_2}\\
&\quad + \frac{1}{4}|V\rangle_1\,(|H\rangle + |V\rangle)_2 \otimes (|0000\rangle + |0011\rangle - |1100\rangle - |1111\rangle)_{a_1b_1a_2b_2}.
\end{aligned} \tag{20}$$

Second, the two parts of photon 1 are rejoined at $PBS_4$ and travel through a $PBS\pm$. Meanwhile, the photon 2 at Bob's place has the same process as photon 1 in Alice simultaneously. After the above

**Table 2**
The results of the four single-photon detectors corresponding to the initial entangled states of the four atoms.

| Initial $(a_1b_1)$ | States $(a_2b_2)$ | Photons measurement Detector click |
|---|---|---|
| $\|\phi^+\rangle$ | $\|\phi^+\rangle$ | $D_2D_4$ or $D_1D_3$ |
| $\|\phi^+\rangle$ | $\|\psi^+\rangle$ | $D_2D_3$ or $D_1D_4$ |
| $\|\psi^+\rangle$ | $\|\phi^+\rangle$ | $D_2D_3$ or $D_1D_4$ |
| $\|\psi^+\rangle$ | $\|\psi^+\rangle$ | $D_2D_4$ or $D_1D_3$ |

interactions, the state of the whole system collapses into $|\Phi_2\rangle$. Here

$$|\Phi_2\rangle = \frac{1}{4}(|H\rangle + |V\rangle)_1(|H\rangle + |V\rangle)_2\,(|0000\rangle + |1111\rangle)_{a_1b_1a_2b_2} + \frac{1}{4}(|H\rangle - |V\rangle)_1(|H\rangle - |V\rangle)_2\,(|0011\rangle + |1100\rangle)_{a_1b_1a_2b_2}. \tag{21}$$

Finally, photon 1 and photon 2 are probed by single-photon detectors.

Similarly, the evolution of the other three cases can be described as follows:

$$\begin{aligned}&\frac{1}{2}(|H\rangle + |V\rangle)_1(|H\rangle + |V\rangle)_2\,|\phi^+\rangle_{a_1b_1}|\psi^+\rangle_{a_2b_2}\\ &\quad\to -\frac{1}{4}(|H\rangle + |V\rangle)_1(|H\rangle - |V\rangle)_2\,(|0001\rangle + |1110\rangle)_{a_1b_1a_2b_2}\\ &\qquad -\frac{1}{4}(|H\rangle - |V\rangle)_1(|H\rangle + |V\rangle)_2\,(|0010\rangle + |1101\rangle)_{a_1b_1a_2b_2},\end{aligned} \tag{22}$$

$$\begin{aligned}&\frac{1}{2}(|H\rangle + |V\rangle)_1(|H\rangle + |V\rangle)_2\,|\psi^+\rangle_{a_1b_1}|\phi^+\rangle_{a_2b_2}\\ &\quad\to \frac{1}{4}(|H\rangle + |V\rangle)_1(|H\rangle - |V\rangle)_2\,(|0100\rangle + |1011\rangle)_{a_1b_1a_2b_2}\\ &\qquad +\frac{1}{4}(|H\rangle - |V\rangle)_1(|H\rangle + |V\rangle)_2\,(|0111\rangle + |1000\rangle)_{a_1b_1a_2b_2},\end{aligned} \tag{23}$$

and

$$\begin{aligned}&\frac{1}{2}(|H\rangle + |V\rangle)_1(|H\rangle + |V\rangle)_2\,|\psi^+\rangle_{a_1b_1}|\psi^+\rangle_{a_2b_2}\\ &\quad\to -\frac{1}{4}(|H\rangle + |V\rangle)_1(|H\rangle + |V\rangle)_2\,(|0101\rangle + |1010\rangle)_{a_1b_1a_2b_2}\\ &\qquad -\frac{1}{4}(|H\rangle - |V\rangle)_1(|H\rangle - |V\rangle)_2\,(|0110\rangle + |1001\rangle)_{a_1b_1a_2b_2}.\end{aligned} \tag{24}$$

The measurement results of all cases are shown in Table 2. With the outcomes of four detectors, we can distill $|\phi^+\rangle_{a_1b_1}|\phi^+\rangle_{a_2b_2}$ and $|\psi^+\rangle_{a_1b_1}|\psi^+\rangle_{a_2b_2}$ from the four cases mentioned above.

Third, to recover the entangled states of atoms $a_1$ and $b_1$, Alice and Bob should perform a Hadamard operation $H_a$ on the two nonlocal atoms $a_2$ and $b_2$ in the waveguides, respectively. Then, Alice and Bob measure the states of the two atoms $a_2$ and $b_2$, and compare their results with the help of classical communication. If the results are the same ones, nothing needs to be done; otherwise, a $\sigma_z$ operation needs to be put on atom $a_1$. From Table 2, one can see that there are two cases in the reserved entangled pairs $a_1$ and $b_1$. One is $|\phi^+\rangle_{a_1b_1}$ with a probability of $F^2$, and the other one is $|\psi^+\rangle_{a_1b_1}$ with a probability of $(1-F)^2$. Therefore, in the filtered states, the probability of $|\phi^+\rangle_{a_1b_1}$ is $F' = \frac{F^2}{F^2+(1-F)^2}$. That is, after the purification process, the fidelity of $|\phi^+\rangle_{a_1b_1}$ becomes $F'$. When $F > \frac{1}{2}$, one can easily get $F' > F$.

## 4. Discussion and summary

We have proposed a heralded scheme for quantum repeater, including robust nonlocal entanglement creation against collective noise, entanglement swapping, and entanglement purification modules. The key element in our protocol is the scattering process between photons and atoms in 1D waveguides. In the following section, we will discuss the performance of our quantum repeater under practical conditions, defining $p_s = |\langle\psi|\phi_r\rangle|^2$ as the success probability of the scattering event in the heralded protocol, as shown in Fig. 1(b). Here $|\psi\rangle$ and $|\phi_r\rangle$ are the spatial wave functions of the incident photon and the reflected photon component after the scattering event, respectively. For perfect scattering event, i.e., with $P \to \infty$, $|\phi_r\rangle = -|\psi\rangle$, and the success probability $p_s$ is 100%. Whereas, in realistic situations, with finite $P$, $|\phi_r\rangle \neq -|\psi\rangle$, it includes two cases: one is the successful event of imperfect processes, where the polarization of output photon is changed but $|\phi_r\rangle = r|\psi\rangle$ ($|r| < 1$); the other one is that the scattering event between atoms and photons does not happen at all. For the latter case, the output photons with unchanged polarization are detected at the entrance, and the corresponding quantum computation is discarded. Assuming that the linear optical elements are perfect in our protocols, the heralded mechanism ensures that the faulty events cannot influence the fidelity of our scheme, but decrease the efficiency, because the success probability $p_s$ is determined by the quality of the atom-waveguide systems.

As mentioned above, a high Purcell factor is needed in our scheme, which can effectively improve the performance of our protocols. In the last decade, great progress has been made in the emitter–waveguide systems in both theory and experiment. In 2005, Vlasov et al. [52] experimentally demonstrated that a Purcell factor approaching 60 can be observed in low-loss silicon photonic crystal waveguides. In 2006, Chang et al. [53] presented a scheme that a dipole emitter is coupled to a nanowire or a metallic nanotip, in which a Purcell factor $P = 5.2 \times 10^2$ is theoretically obtained for a silver nanowire. Subsequently, using the surface plasmons of a conducting nanowire, Chang et al. [54] proposed a method to obtain an effective Purcell factor, which can reach $10^3$ in realistic systems in principle. In addition, short waveguide lengths of only 10 to 20 unit cells were theoretically found by Manga Rao and Hughes [55] to produce a very large Purcell factor in 2007, and the experimental progress on short photonic crystal waveguides was reported by Dewhurst et al. [56] and Hoang et al. [57]. Later, based on subwavelength confinement of optical fields near metallic nanostructures, Akimov et al. [58] demonstrated a broadband approach for manipulating photon–emitter interactions. In 2008, photonic crystal waveguides were exploited by Hansen et al. [59] to enable single quantum dots to exhibit nearly perfect spontaneous emission into the guided modes ($\gamma_{1D} \gg \gamma'$), where the light–matter coupling strength is largely enhanced. In 2010, a Purcell factor of $P = 5.2$ was experimentally observed for single quantum dots coupled to a photonic crystal waveguide [60]. In 2012, Goban [61] reported the experimental implementation of a state-insensitive, compensated optical trap for single Cs atoms, which provides the precise atomic spectroscopy near dielectric surfaces. Moreover, in 2013, Hung et al. [62] proposed a protocol that one atom trapped in single nanobeam structure could provide a resonant probe with transmission $|t|^2 \leq 10^{-2}$ in theory. A similar scheme was realized in experiment by Goban et al. [63] in 2014. Recently, due to the coupling of a single emitter to a dielectric slot waveguide, a high Purcell factor $P = 31$ was also observed by Kolchin et al. [64] in experiment.

As illustrated in Section 2, we can obtain the reflection coefficient for an incident photon scattering with an atom in the 1D waveguide. On resonance, $r = -1/(1+1/P)$, and we get the relation between the success probability $p_s$ (i.e., $|r|^2$) and the Purcell factor $P$, as shown in Fig. 5(a). Moreover, the scattering quality is also influenced by the nonzero photonic detuning, and the details are described in Fig. 5(b), where $p_s$ is plotted as a function of the detuning parameter $\Delta/\gamma_{1D}$. From Fig. 5, one can see that the success probability $p_s$ would exceed 90% on the condition that the Purcell factor $P \geq 50$ and the detuning parameter $\Delta/\gamma_{1D} \leq 0.13$, which could be achievable in realistic systems. For instance, when we choose $P = 100$ and $\Delta = 0.1\gamma_{1D}$ for atom-waveguide systems, the success probability $p_s$ of the scattering process in Fig. 1(b) can reach 94.33%. In our protocols, the faulty events between photons and atomic qubits can be heralded by single-photon detectors. However, the imperfection coming from photon loss is still an inevitable problem in our scheme. The photon loss is caused by various drawbacks, such as the fiber absorption, the imperfection of 1D waveguides, and the inefficiency of the

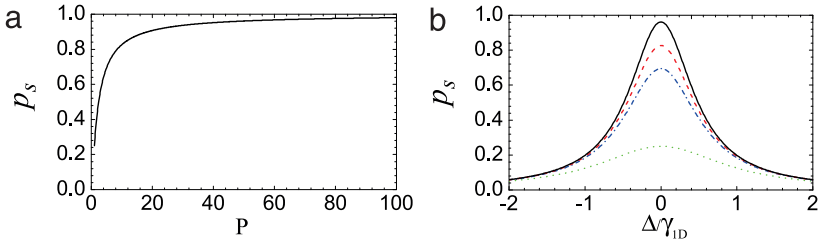


**Fig. 5.** (Color online) The success probability $p_s$ of the scattering process vs. the Purcell factor $P$ and the detuning parameter $\Delta/\gamma_{1D}$. (a) The success probability $p_s$ vs. the Purcell factor $P$ when the detuning $\Delta = 0$. (b) The success probability $p_s$ vs. the parameters $\Delta/\gamma_{1D}$. The dotted (green), dashed–dotted (blue), dashed (red), and solid (black) lines correspond to $P = 1$, $P = 5$, $P = 10$, $P = 50$, respectively.

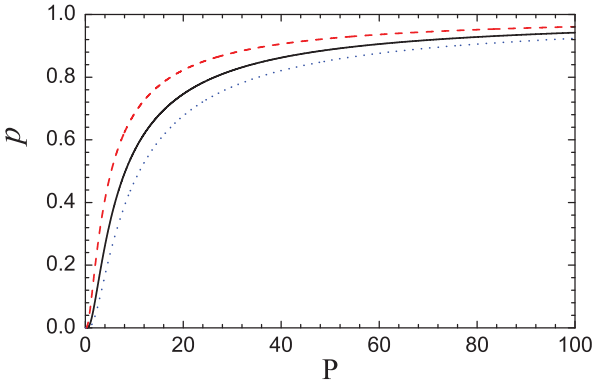


**Fig. 6.** (Color online) The success probabilities of our entanglement creation (solid line, black), entanglement swapping (dashed line, red), entanglement purification (dotted line, blue) protocols vs. the Purcell factor $P$. Here, the detuning parameter is $\Delta = 0$.

single-photon detectors. In fact, if optical losses appear in the prediction of faulty events, the fidelities of our protocols cannot be unity as faulty scattering events will not always be detected. Recently, many proposals have been presented to solve the problems of photon loss [65–68].

Provided that the linear optical elements are perfect in our scheme, due to the heralded mechanism, only when no faulty scattering events are detected in our protocols, can we obtain the quantum repeater successfully. Here, the times of the basic scattering event (Fig. 1(b)) occurred in our entanglement creation, swapping, and purification protocols are three, two, and four, respectively. We calculate the success probabilities of our entanglement creation, swapping, and purification protocols as a function of the Purcell factor $P$, as shown in Fig. 6. Recently, Arcari et al. [69] exploited the photonic crystal waveguide to experimentally realize near-unity coupling efficiency of a quantum dot to the waveguide mode. In their experiment, the decay rate of the quantum dot into the waveguide is $\gamma_{1D} = 6.182$ GHz, and the decay rate of the quantum emitter into free space and all other modes is $\gamma' = 98$ MHz, which indicates that the Purcell factor $P = 63.1$ can be implemented. The resonance frequency of the quantum dot is $\omega_a = 2 \times 10^6$ GHz. With these experimental parameters mentioned above, we can obtain the success probabilities of our entanglement creation, swapping, and purification protocols are $p_1 = 91.00\%$, $p_2 = 93.90\%$, and $p_3 = 88.18\%$, respectively, when the detuning parameter is $\Delta = 0$. With the remarkable progress in photonic nanostructures [70], our protocols for the heralded quantum repeater may be experimentally feasible in the near future.

Compared with other schemes, the protocols we present for the heralded quantum repeater have some interesting features. First, the faulty events caused by frequency mismatches, weak coupling, atomic decay into free space, or finite bandwidth of the incident photon can be turned into detection of the output photon polarization, and that just affects the efficiency of our protocols, not the fidelity. In other words, our scheme either succeeds with a perfect fidelity or fails in a heralded way, which is an

advantageous feature for quantum communication. Second, our scheme focuses on 1D waveguides, in which the modes can be highly dispersive. In a waveguide, the quantum emitter can efficiently couple single photon to the propagating modes over a wide bandwidth, which provides an alternative to the high-Q cavity case for enhancing light–matter interaction. Third, motivated by recent experimental progress, our scheme for the heralded quantum repeater is feasible in some other quantum systems, such as superconducting quantum circuit coupled to transmission lines [71], quantum dot embedded in a nanowire [72], and photonic crystal waveguide with quantum dots [70].

In summary, we have proposed a heralded quantum repeater based on the scattering of photons off single emitters in 1D waveguides. The information of the entangled states is encoded on four-level atoms embedded in 1D waveguides. As our protocols can transform faulty events into the detection of photon polarization, we present a different way for constructing quantum repeaters in solid-state quantum systems. With the significant progress on manipulating atom-waveguide systems, our quantum repeater may be very useful for quantum communication in the future.

## Acknowledgments

This work was supported by the National Natural Science Foundation of China under Grant Nos. 11674033, 11475021, 11505007, and 11474026, the Fundamental Research Funds for the Central Universities under Grant No. 2015KJJCA01, the National Key Basic Research Program of China under Grant No. 2013CB922000, the Youth Scholars Program of Beijing Normal University under Grant No. 2014NT28, and the Open Research Fund Program of the State Key Laboratory of Low-Dimensional Quantum Physics, Tsinghua University Grant No. KF201502.

## References

[1] A.K. Ekert, Phys. Rev. Lett. 67 (1991) 661.
[2] C.H. Bennett, G. Brassard, N.D. Mermin, Phys. Rev. Lett. 68 (1992) 557.
[3] M. Hillery, V. Buzek, A. Berthiaume, Phys. Rev. A 59 (1999) 1829.
[4] G.L. Long, X.S. Liu, Phys. Rev. A 65 (2002) 032302.
[5] F.G. Deng, G.L. Long, X.S. Liu, Phys. Rev. A 68 (2003) 042317.
[6] H.J. Briegel, W. Dür, J.I. Cirac, P. Zoller, Phys. Rev. Lett. 81 (1998) 5932.
[7] M. Zukowski, A. Zeilinger, M.A. Horne, A.K. Ekert, Phys. Rev. Lett. 71 (1993) 4287.
[8] C.H. Bennett, G. Brassard, S. Popescu, B. Schumacher, J.A. Smolin, W.K. Wootters, Phys. Rev. Lett. 76 (1996) 722.
[9] C. Simon, J.W. Pan, Phys. Rev. Lett. 89 (2002) 257901.
[10] Y.B. Sheng, F.G. Deng, H.Y. Zhou, Phys. Rev. A 77 (2008) 042308.
[11] Y.B. Sheng, F.G. Deng, Phys. Rev. A 81 (2010) 032307.
[12] Y.B. Sheng, F.G. Deng, Phys. Rev. A 82 (2010) 044305.
[13] X.H. Li, Phys. Rev. A 82 (2010) 044304.
[14] F.G. Deng, Phys. Rev. A 83 (2011) 062316.
[15] B.C. Ren, F.F. Du, F.G. Deng, Phys. Rev. A 90 (2014) 052309.
[16] G.Y. Wang, Q. Liu, F.G. Deng, Phys. Rev. A 94 (2016) 032319.
[17] F.F. Du, T. Li, G.L. Long, Ann. Phys. 375 (2016) 105.
[18] F.G. Deng, B.C. Ren, X.H. Li, Sci. Bull. 62 (2017) 46.
[19] L.M. Duan, M.D. Lukin, J.I. Cirac, P. Zoller, Nature 414 (2001) 413.
[20] A. Klein, U. Dorner, C.M. Alves, D. Jaksch, Phys. Rev. A 73 (2006) 012332.
[21] B. Zhao, Z.B. Chen, Y.A. Chen, J. Schmiedmayer, J.W. Pan, Phys. Rev. Lett. 98 (2007) 240502.
[22] T. Li, G.J. Yang, F.G. Deng, Phys. Rev. A 93 (2016) 012302.
[23] T. Li, F.G. Deng, Sci. Rep. 5 (2015) 15610.
[24] Z. Zhao, T. Yang, Y.A. Chen, A.N. Zhang, J.W. Pan, Phys. Rev. Lett. 90 (2003) 207901.
[25] A. Kuzmich, W.P. Bowen, A.D. Boozer, A. Boca, C.W. Chou, L.M. Duan, H.J. Kimble, Nature 423 (2003) 731.
[26] Z.S. Yuan, Y.A. Chen, B. Zhao, S. Chen, J. Schmiedmayer, J.W. Pan, Nature 454 (2008) 1098.
[27] N. Curtz, R. Thew, C. Simon, N. Gisin, H. Zbinden, Opt. Express 18 (2010) 22099.
[28] N. Sangouard, C. Simon, H. de Riedmatten, N. Gisin, Rev. Modern Phys. 83 (2011) 33.
[29] K. Hammerer, A.S. Sørensen, E.S. Polzik, Rev. Modern Phys. 82 (2010) 1041.
[30] J.I. Cirac, P. Zoller, H.J. Kimble, H. Mabuchi, Phys. Rev. Lett. 78 (1997) 3221.
[31] T. Wilk, S.C. Webster, H.P. Specht, G. Rempe, A. Kuhn, Phys. Rev. Lett. 98 (2007) 063601.
[32] D.L. Moehring, P. Maunz, S. Olmschenk, K.C. Younge, D.N. Matsukevich, L.M. Duan, C. Monroe, Nature 449 (2007) 68.
[33] Y. Li, L. Aolita, L.C. Kwek, Phys. Rev. A 83 (2011) 032313.
[34] J.T. Shen, S. Fan, Opt. Lett. 30 (2005) 2001.
[35] D.E. Chang, A.S. Sørensen, E.A. Demler, M.D. Lukin, Nat. Phys. 3 (2007) 807.
[36] I. Söllner, S. Mahmoodian, S.L. Hansen, L. Midolo, A. Javadi, G. Kiršanské, T. Pregnolato, H. El-Ella, E.H. Lee, J.D. Song, S. Stobbe, P. Lodahl, Nat. Nanotechnol. 10 (2015) 775.
[37] K. Kojima, H.F. Hofmann, S. Takeuchi, K. Sasaki, Phys. Rev. A 68 (2003) 013803.

[38] M.C. Kuzyk, S.J. van Enk, H. Wang, Phys. Rev. A 88 (2013) 062341.
[39] T.C.H. Liew, V. Savona, Phys. Rev. A 85 (2012) 050301.
[40] M. Bajcsy, S. Hofferberth, V. Balic, T. Peyronel, M. Hafezi, A. Zibrov, V. Vuletic, M.D. Lukin, Phys. Rev. Lett. 102 (2009) 203902.
[41] B.C. Ren, F.G. Deng, Sci. Rep. 4 (2014) 4623.
[42] B.C. Ren, G.Y. Wang, F.G. Deng, Phys. Rev. A 91 (2015) 032328.
[43] Y. Li, L. Aolita, D.E. Chang, L.C. Kwek, Phys. Rev. Lett. 109 (2012) 160504.
[44] E. Waks, J. Vuckovic, Phys. Rev. Lett. 96 (2006) 153601.
[45] J.H. An, M. Feng, C.H. Oh, Phys. Rev. A 79 (2009) 032303.
[46] D. Kalamidas, Phys. Lett. A 343 (2005) 331.
[47] T. Yamamoto, J. Shimamura, S.K. Özdemir, M. Koashi, N. Imoto, Phys. Rev. Lett. 95 (2005) 040503.
[48] X.H. Li, F.G. Deng, H.Y. Zhou, Appl. Phys. Lett. 91 (2007) 144101.
[49] S. Mahmoodian, P. Lodahl, A.S. Sørensen, arXiv:1602.07054.
[50] J. Berezovsky, M.H. Mikkelsen, N.G. Stoltz, L.A. Coldren, D.D. Awschalom, Science 320 (2008) 349.
[51] D. Press, T.D. Ladd, B.Y. Zhang, Y. Yamamoto, Nature 456 (2008) 218.
[52] Y.A. Vlasov, M. O'Boyle, H.F. Hamann, S.J. McNab, Nature 438 (2005) 65.
[53] D.E. Chang, A.S. Sørensen, P.R. Hemmer, M.D. Lukin, Phys. Rev. Lett. 97 (2006) 053002.
[54] D.E. Chang, A.S. Sørensen, P.R. Hemmer, M.D. Lukin, Phys. Rev. B 76 (2007) 035420.
[55] V.S.C. Manga Rao, S. Hughes, Phys. Rev. Lett. 99 (2007) 193901.
[56] S.J. Dewhurst, D. Granados, D.J.P. Ellis, A.J. Bennett, R.B. Patel, I. Farrer, D. Anderson, G.A.C. Jones, D.A. Ritchie, A.J. Shields, Appl. Phys. Lett. 96 (2010) 031109.
[57] T. Ba Hoang, J. Beetz, L. Midolo, M. Skacel, M. Lermer, M. Kamp, S. Höfling, L. Balet, N. Chauvin, A. Fiore, Appl. Phys. Lett. 100 (2012) 061122.
[58] A.V. Akimov, A. Mukherjee, C.L. Yu, D.E. Chang, A.S. Zibrov, P.R. Hemmer, H. Park, M.D. Lukin, Nature 450 (2007) 402.
[59] T. Lund-Hansen, S. Stobbe, B. Julsgaard, H. Thyrrestrup, T. Sünner, M. Kamp, A. Forchel, P. Lodahl, Phys. Rev. Lett. 101 (2008) 113903.
[60] H. Thyrrestrup, L. Sapienza, P. Lodahl, Appl. Phys. Lett. 96 (2010) 231106.
[61] A. Goban, K.S. Choi, D.J. Alton, D. Ding, C. Lacroûte, M. Pototschnig, T. Thiele, N.P. Stern, H.J. Kimble, Phys. Rev. Lett. 109 (2012) 033603.
[62] C.L. Hung, S.M. Meenehan, D.E. Chang, O. Painter, H.J. Kimble, New J. Phys. 15 (2013) 083026.
[63] A. Goban, C.L. Hung, S.P. Yu, J.D. Hood, J.A. Muniz, J.H. Lee, M.J. Martin, A.C. McClung, K.S. Choi, D.E. Chang, O. Painter, H.J. Kimble, Nature Commun. 5 (2014) 3808.
[64] P. Kolchin, N. Pholchai, M.H. Mikkelsen, J. Oh, S. Ota, M.S. Islam, X.B. Yin, X. Zhang, Nano Lett. 15 (2015) 464.
[65] N. Gisin, S. Pironio, N. Sangouard, Phys. Rev. Lett. 105 (2010) 070501.
[66] S. Kocsis, G.Y. Xiang, T.C. Ralph, G.J. Pryde, Nat. Phys. 9 (2012) 23.
[67] C.I. Osorio, N. Bruno, N. Sangouard, H. Zbinden, N. Gisin, R.T. Thew, Phys. Rev. A 86 (2012) 023815.
[68] T.J. Wang, C. Cao, C. Wang, Phys. Rev. A 89 (2014) 052303.
[69] M. Arcari, I. Söllner, A. Javadi, S. Lindskov Hansen, S. Mahmoodian, J. Liu, H. Thyrrestrup, E.H. Lee, J.D. Song, S. Stobbe, P. Lodahl, Phys. Rev. Lett. 113 (2014) 093603.
[70] P. Lodahl, S. Mahmoodian, S. Stobbe, Rev. Modern Phys. 87 (2015) 347.
[71] A.F. van Loo, A. Fedorov, K. Lalumiére, B.C. Sanders, A. Blais, A. Wallraff, Science 342 (2013) 1494.
[72] M. Munsch, J. Claudon, J. Bleuse, N.S. Malik, E. Dupuy, J.M. Gérard, Y. Chen, N. Gregersen, J. Mork, Phys. Rev. Lett. 108 (2012) 077405.